HHS Public Access

Author manuscript

J Mol Biol. Author manuscript; available in PMC 2017 October 09.

Published in final edited form as:

J Mol Biol. 2016 October 9; 428(20): 4168–4184. doi:10.1016/j.jmb.2016.08.011.

A Conserved Cysteine within the ATPase Domain of the Endoplasmic Reticulum Chaperone BiP is Necessary for a Complete Complement of BiP Activities

Mengni Xu, **Heather M. Marsh**, and **Carolyn S. Sevier**

Department of Molecular Medicine, Cornell University, Ithaca, NY 14853

Abstract

Among the amino acids, cysteine stands apart based on its highly reactive sulfur group. In general, cysteine is underrepresented in proteins. Yet when present, the features of cysteine often afford unique function. We have shown previously that a cysteine within the ATPase domain of yeast BiP (Kar2) serves as a sensor of the endoplasmic reticulum (ER) redox environment [1, 2]. Under conditions of increased oxidant (oxidative stress) this cysteine becomes oxidized, changing Kar2 from an ATP-dependent foldase to an ATP-independent holdase. We were struck by the high degree of conservation for this cysteine between BiP orthologs, and we sought to determine how cysteine substitution impacts Kar2 function. We observed no single amino acid replacement is capable of recreating the range of functions that can be achieved by wild-type Kar2 with its cysteine in either the unmodified or oxidized states. However, we were able to generate mutants that could selectively replicate the distinct activities exhibited by either unmodified or oxidized Kar2. We found that the ATPase activity displayed by unmodified Kar2 is fully maintained when Cys63 is replaced with Ala or Val. Conversely, we demonstrate that several amino acid substitutions (including His, Phe, Pro, Trp, Tyr) support an enhanced viability during oxidative stress associated with oxidized Kar2, although these alleles are compromised as an ATPase. We reveal the range of activity demonstrated by wild-type Kar2 can be replicated by co-expression of Kar2 mutants that mimic either the unmodified or oxidized Kar2 state, allowing for growth during standard and oxidative stress conditions.

Graphical abstract

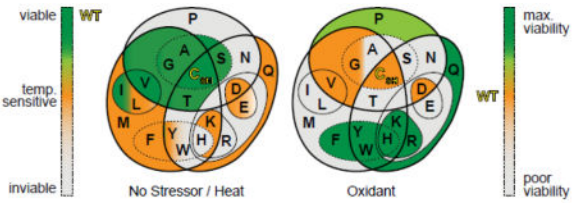

To whom correspondence should be addressed: Carolyn Sevier, Department of Molecular Medicine, Cornell University, VMC C4-141, Ithaca, NY 14853, Phone: 607-253-3657, css224@cornell.edu.

Keywords

Hsp70; Kar2; heat shock; oxidative stress; redox signaling

INTRODUCTION

BiP is an abundant and essential molecular chaperone of the Hsp70 family located in the lumen of the endoplasmic reticulum (ER). BiP consists of two functional domains: a nucleotide-binding domain (NBD), which binds and hydrolyzes ATP, and a substrate-binding domain (SBD), which binds polypeptides. In cells, BiP associates with unfolded polypeptides, exhibiting a preference toward short amino acid sequences enriched in aliphatic residues [3]. Unfolded polypeptides associate with the SBD, and polypeptide binding is controlled through the ATPase activity of the NBD.

BiP serves several fundamental roles that together work to maintain ER homeostasis (for recent reviews see [4, 5]). BiP plays an early role in secretory protein biogenesis; BiP binds nascent polypeptide chains to facilitate their translocation across the ER membrane [6, 7]. Once polypeptides arrive in the ER lumen, BiP serves to limit polypeptide misfolding and/or aggregation by binding the exposed hydrophobic segments of unfolded proteins, maintaining these proteins in a folding competent state. In addition, BiP facilitates the clearance of damaged lumenal proteins by assisting their movement across the translocon into the cytoplasm for degradation by the proteasome [8–11]. Moreover, BiP functions as an important physical component of the Sec61 translocon, acting as a molecular gate to control the movement of small molecules across the aqueous translocation pore to maintain critical ion gradients (e.g. calcium stores) [12].

Cells contain several means to regulate BiP activity to buffer against fluctuations in the ER folding load. These systems serve to augment (or down-regulate) BiP chaperone availability to counterbalance a corresponding increase (or decrease) in the burden of unfolded ER polypeptides. A well-established means to modulate BiP activity is the unfolded protein response (UPR), a transcriptional response activated when there is a buildup of unfolded polypeptides in the ER (reviewed in [13]). BiP is a mediator and a target gene of the UPR. The increased chaperone capacity associated with the transcriptional upregulation of BiP (as a consequence of the UPR) serves to supplement the ER folding capacity. BiP chaperone activity can also be tuned through post-translational modification to increase or down-regulate BiP function to appropriately complement the existing ER folding load. Several post-translational modifications have been suggested to regulate BiP activities, including AMPylation [14–16] and oligomerization [17]. In addition, it has been proposed that BiP is ADP-ribosylated [18, 19] and phosphorylated [19], although it has been put forward that these two postulated modifications may reflect misattributed AMPylation events [15].

A recently reported example of post-translational tuning of BiP activity that captured our attention centers on a conserved cysteine within the BiP ATPase domain. It has been demonstrated for both mammalian and yeast BiP that during conditions of increased ER oxidation, this cysteine becomes oxidized, which in turn augments BiP chaperone activity [1, 2, 20]. Such an alteration in BiP activity is thought to benefit cells during oxidative stress

by limiting polypeptide aggregation during suboptimal redox conditions for ER protein folding. In yeast, the conserved BiP (Kar2) cysteine undergoes modification by peroxide and/or glutathione, forming a sulfenic acid or glutathione adduct [1, 2]. In mammals (mice), the equivalent cysteine forms an intramolecular disulfide bond (with a second BiP cysteine) during overly oxidizing conditions [20].

We were struck by the high degree of conservation for the conserved redox-active BiP cysteine across species. A BLAST search [21] of the non-redundant NCBI protein database for BiP orthologs revealed the vast majority of predicted BiP proteins contain a cysteine at the equivalent position to the redox-active cysteine characterized in *S. cerevisiae* and *M. musculus* BiP (Figure 1). Strikingly, we observed the redox-active cysteine was maintained in BiP proteins with relatively low sequence conservation, such as human and microsporidia (*E. cuniculi*) BiP that share only 30% sequence identity. Notably, although the vast majority of sequences we identified in our BLAST search contained a conserved cysteine, we did observe outlier sequences lacking the cysteine in trypanosomes and entamoebae, which have been described previously [22, 23] (two such sequences are included in Figure 1). Of interest, the second cysteine in mouse BiP involved in forming the intramolecular disulfide also appears conserved selectively among the vertebrate BiP orthologs (Figure 1).

It has been reported that, in comparison to the other standard amino acids, cysteine shows an extreme conservation pattern; cysteine residues are either highly or poorly conserved between orthologous proteins [24]. Highly conserved cysteines are most often located in functionally important sites in proteins, such as catalytic active sites, whereas surface-exposed cysteines are poorly retained [24]. Thus, it seems likely the conservation of the BiP cysteine speaks to its importance in BiP activity and cell function.

Here we sought to learn more about the importance of the conserved cysteine for BiP activity, focusing on *S. cerevisiae* BiP (Kar2) as a model BiP ortholog. Of note, Kar2 contains only one cysteine (the single redox-active Cys63). In prior limited mutagenesis studies of the Kar2 cysteine, we observed a complex relationship between the cysteine and the various known BiP activities. When the Kar2 Cys63 was replaced with alanine, Kar2 ATPase activity was retained, yet this mutation limited the viability of cells during conditions of increased ER oxidation [1]. We attributed the increased sensitivity to oxidative stress to the loss of cysteine post-translational oxidation upon replacement of the Kar2 cysteine with alanine [1]. Conversely, we observed replacement of the Kar2 cysteine with an amino acid containing a charged (Asp) or large (Phe, Tyr, Trp) side chain could recapitulate the beneficial phenotypes observed for modified (oxidized) BiP during oxidative stress, yet these Kar2 alleles showed limited ATPase activity [1]. Here we report an expanded mutagenesis study, which includes replacement of the Kar2 cysteine with each of the common amino acids. We identify five new Kar2 alleles (Kar2-C63H/K/P/Q/R) that, like Kar2-C63F/Y/W, show a loss of ATPase activity yet recapitulate the protection against oxidative stress observed with oxidized wild type Kar2. We also describe a new class of Kar2 cysteine mutants that show limited ATPase activity yet do not significantly protect cells during oxidative stress (Kar2-C63E/N). Under non-stress conditions, we find cysteine-to-alanine or cysteine-to-valine substitution mutants are the two alleles that exhibit the least

perturbation of ER homeostasis. Intriguingly, these are the amino acids found in place of cysteine in the entamoeba and trypanosomal BiP proteins (Figure 1).

RESULTS

Kar2 cysteine mutants differ in their ability to provide essential cell function

KAR2 is an essential gene in yeast. To determine how replacement of the conserved Kar2 cysteine impacts the essential cellular function of Kar2, we tested whether *kar2* Cys63 amino acid replacement alleles could serve as the sole copy of cellular *KAR2*. We observed that essential Kar2 function is retained (yeast are viable) when Cys63 is replaced with an amino acid that contains a relatively small side chain, including a small hydrophobic (A/G), aliphatic side (I/V), or polar (S/T) side chain (Figure 2a). Yeast strains containing these alleles also appeared competent for growth during heat stress, exhibiting a growth pattern identical to wild-type cells at high temperature (Figure 2b). However, all other cysteine replacement mutants showed a loss of essential Kar2 activity. Larger nonpolar (L/M) and polar (N/Q) amino acid substitution mutants exhibited either a complete loss of essential Kar2 function (*kar2-C63N*) (Figure 2a) or a compromised ability to serve as the sole copy of Kar2, as evidenced by a decreased viability at high temperature (*kar2-C63L/M/Q*) (Figure 2b). Similarly, substitution of the cysteine with a charged amino acid impaired function. As we reported previously, a strain containing *kar2-C63D* as the sole *KAR2* allele was compromised for viability at high temperature (Figure 2b) [1]. Replacement of the Kar2 cysteine with the charged amino acids E/K/H/R also impacted cell viability, resulting in no cell growth (*kar2-C63H/R)* (Figure 2a) or temperature-sensitive growth *(kar2-C63E/K)* (Figure 2b). In addition, replacement of the cysteine with amino acids containing aromatic side chains generated alleles with a compromised ability to serve as the sole copy of Kar2 [1]; a *kar2-C63W* allele was unable to support any growth (Figure 2a) while *kar2-C63F/Y* alleles were viable but temperature sensitive for growth (Figure 2b). A *kar2-C63P* allele was also unable to complement yeast containing a *KAR2* chromosomal deletion (Figure 2a); the structure of the Kar2 ATPase domain shows Cys63 located within a beta-sheet [25], and it seems likely the inability of the *kar2-C63P* allele to support yeast viability relates to a disruption of this beta-sheet as a byproduct of the conformational rigidity associated with proline.

Kar2 normally facilitates the translocation of nascent polypeptides into the ER lumen. We observed that all the Kar2 mutant strains showing a temperature sensitive growth phenotype (Figure 2b) also exhibited a defect in polypeptide translocation. An accumulation of untranslocated polypeptides after a brief (60 min) shift to 37°C was readily observed in *kar2*Δ strains supporting a single copy plasmid for *kar2-C63F/K/L/M/Q/Y* (Figure 3). An attenuation of polypeptide translocation was also seen for strains with a *kar2-C63D* or *kar2-C63E* plasmid after a shift to high temperature (Figure 3), yet the level of precursor accumulation observed for these strains was modest relative to the other temperature-sensitive yeast strains. Untranslocated proteins were distinguished by an absence of the characteristic size shifts associated with post-translational processing events that take place in the ER lumen, including the decrease in size associated with signal sequence cleavage (Kar2), and the increase in mobility associated with glycosylation (PDI) (Figure 3).

ER stress is observed in cells containing Kar2 cysteine substitution alleles that otherwise lack obvious growth defects

In keeping with a loss of vital Kar2 activity, the strains showing a temperature-sensitive growth defect also exhibited an approximately three-fold induction of the UPR at 37°C (Figure 4a). UPR levels in the mutant strains at 37°C were comparable to those observed in cells treated with dithiothreitol (DTT), a known UPR inducer (Figure 4a). Interestingly, a robust UPR induction was observed for the *kar2-C63D/E* strains (Figure 4a) that appeared only mildly deficient for protein translocation into the ER (Figure 3); the increased level of Kar2 and/or other chaperones upon UPR induction may compensate for any loss of function for the *kar2-C63D/E* alleles in polypeptide translocation. An elevated UPR at 37°C was also seen in strains containing *kar2-C63G, kar2-C63I, kar2-C63S, kar2-C63T* (Figure 4b), which show no obvious temperature-sensitive growth or translocation defects (Figure 2, 3). These data suggest the Kar2-C63G/I/S/T proteins are modestly compromised for Kar2 activity, which may also be compensated for by cellular effectors and/or increased levels of Kar2 as a byproduct of UPR induction.

Only alanine and valine substitution alleles retain wild-type Kar2 ATPase activity in vitro

Given the subtle loss of Kar2 function implied by the increased UPR induction in strains with *kar2-C63G/I/S/T* alleles (which otherwise appeared wild-type; Figure 2–4), we sought to more directly assess the impact of cysteine substitution on Kar2 ATPase activity. To monitor ATPase activity, we purified recombinant wild-type and Kar2 cysteine mutants from *E. coli* and assayed their ATPase activity *in vitro*.

As anticipated, recombinant protein containing the same mutations that were unable support growth of yeast (Figure 2a) showed negligible hydrolysis of ATP in vitro (Figure 5a). In cells, Kar2 ATP hydrolysis and nucleotide exchange are stimulated by J-proteins (Hsp40s) and nucleotide exchange factors (NEFs), respectively. While addition of recombinant J-protein (GST-Sec63J) and recombinant NEF (Lhs1) stimulated the rate of ATP hydrolysis for wild-type Kar2, no significant stimulation was observed for these ATPase compromised alleles in the presence of either J-protein alone or in combination with Lhs1 (Figure 5d).

Recombinant proteins with amino acid substitutions resulting in temperature-sensitive growth defects for yeast cells also showed a severe loss of basal (Figure 5b) and stimulated (Figure 5e) ATP hydrolysis relative to wild-type Kar2. An exception was the Kar2-C63L protein, which showed a loss of basal ATPase activity yet was capable of stimulated ATP hydrolysis in the presence of the recombinant J-protein (Figure 5b, 5e). However, the ATP hydrolysis observed with Kar2-C63L plus Sec63J was not further stimulated upon addition of Lhs1; instead, an inhibition of ATP hydrolysis was observed in the presence of Lhs1 (Figure 5e). Similarly, we observed that addition of Lhs1 inhibited the modest J-protein stimulated ATP hydrolysis observed with Kar2-C63M and Kar2-C63Q (Figure 5e). We have observed that high levels of Lhs1 can lead to inhibition of wild-type Kar2 activity (data not shown). Based on what has been observed for other Hsp70 NEFs, we expect this inhibition reflects a rate of nucleotide release (ATP and ADP) stimulated by Lhs1 that is faster than the rate of nucleotide hydrolysis [26, 27]. Thus these data may reflect a lower apparent affinity of these Kar2 Cys63 mutants for Lhs1.

Interestingly, modest changes in ATPase activity were seen with almost all the recombinant Kar2 proteins that were deemed relatively fit as the sole copy of cellular Kar2 (Figure 2, 3). Indeed, alanine and valine were the only amino acid substitutions that did not disrupt basal Kar2 ATPase activity (Figure 5c). The rate of ATP hydrolysis in the presence of Lhs1 appeared slightly decreased for Kar2-C63V relative to wild-type Kar2 and Kar2-C63A (Figure 5f); it remains to be determined if the slightly lower mean ATPase rate upon Lhs1-stimulation seen for Kar2-C63V is maintained in a larger dataset (29 ± 2 moles ADP generated per mol Kar2-C63V versus 37 ± 2 or 38 ± 2 moles ADP per mol Kar2 or Kar2-C63A) (Figure 5f). Basal ATPase activity was clearly lessened for recombinant Kar2-C63G, Kar2-C63I, Kar2-C63S, and Kar2-C63T proteins (Figure 5c), in keeping with the increased UPR observed for the *kar2-C63G/I/S/T* yeast strains (Figure 4b). However, unlike what we saw for the majority of temperature sensitive yeast *kar2* alleles, the low basal ATPase rates for these Kar2 proteins (G/I/S/T) were effectively stimulated upon the addition of J-protein (Figure 5f). The ability of Sec63 to stimulate the ATPase rate for these proteins *in vivo* may account for the absence of a growth defect in yeast containing these alleles as the only copy of *KAR2* (Figure 2). Reminiscent of Kar2-C63L/M/Q, Kar2-C63I and Kar2-C63T also showed a decreased or unchanged ATP hydrolysis rate, respectively, when reactions were completed in the presence of Lhs1 (Figure 5f). It is intriguing that the Kar2-C63I and Kar2-C63T mutants also showed a greater fold-stimulation with J-protein relative to that observed for wild-type Kar2 (~7-fold versus ~4-fold) (Figure 5f). These data suggest not only an altered interaction with Lhs1 but also a potentially lower affinity of the Kar2-C63I and Kar2-C63T mutants for J-protein.

A subset of the ATPase compromised Kar2 mutants does not undergo an ATP-induced conformational change

Hsp70 proteins have been shown to undergo dynamic structural rearrangements upon the binding and/or hydrolysis of nucleotide. Specifically, it has been observed that ATP binding initiates the opening of a lid that otherwise covers the polypeptide binding site, facilitating peptide release (Figure 6a). A consequence of this structural rearrangement is an alteration in protease accessibility, and this change in protease sensitivity has previously been utilized as a means to monitor the allosteric changes associated with ATP binding in both mammalian and yeast BiP [28–30]. Adopting a similar partial proteolysis scheme, we also observed an ATP-dependent pattern of protease protection for Kar2. Treatment of ATP-bound Kar2 resulted in prominent doublet species running at an apparent molecular weight of ~60 kD (Figure 6c, ATP); the affinity of these fragments for nickel-beads (indicative of the retention of the N-terminal 6xHis tag; data not shown) and the molecular weight of these fragments implies these products result from cleavage within the lid of the Kar2 substrate binding domain, producing lidless Kar2 fragments (Figure 6b). Consistent with this interpretation, ATP was observed to induce a conformational change in mammalian BiP that yielded a similarly sized proteolysis fragment, which was attributed to a cleavage event within the substrate binding domain lid [17]. Full length (FL) Kar2 and an ~ 50 kD band consistent in size with an intact nucleotide binding domain (NBD), which retained the N-terminal 6xHis tag (data not shown), were also observed in the ATP-treated wild-type Kar2 samples, however the intensity of these bands was decreased relative to the prominent 60 kD bands (Figure 6c, ATP). Bands of an even lower abundance with a molecular weight < 37 kD

deduced to be fragments of the substrate binding domain (SBD) were also present in the trypsin-treated wild-type Kar2 samples (Figure 6c, ATP); these bands were unable to bind nickel beads, consistent with the loss of the N-terminal 6xHis tag present in the full length Kar2 (data not shown). In the presence of ADP, similarly sized proteolysis fragments were observed as to those seen for ATP-treated samples, yet the relative abundance of the fragments was altered relative to those observed in the presence of ATP. Proteolyzed wild-type ADP-treated Kar2 showed a decreased level of the lidless Kar2 fragment and a concomitant increase in the recovery of full length Kar2 (Figure 6c, ADP); the decreased recovery of the lidless Kar2 fragment is consistent with an undocking of the SBD from the NBD, protecting the trypsin sites within the lid domain from cleavage. The relative levels of the NBD/SBD bands were also subtly altered in the ADP-treated samples, showing a slight decrease in the NBD fragment and slight increase in the SBD pieces (Figure 6c). In contrast, in the absence of any nucleotide, the only bands observed were the low molecular weight SBD fragments (Figure 6c, no nucleotide); these data suggest the conformational changes associated with nucleotide binding (ATP or ADP) protect the NBD of Kar2 from proteolysis and allow for recovery of fragments containing the NBD (FL, lidless, and NBD products). It is not immediately clear why there is an enhanced recovery of intact SBD fragments in the absence of nucleotide (relative to the ATP or ADP samples), however significant recovery of SBD fragments in the absence of nucleotide provides an additional diagnostic marker for Kar2 nucleotide-dependent conformational changes.

Upon treating the Kar2 cysteine mutants with protease, we observed (unsurprisingly) that the Kar2 Cys63 mutants shown to be most proficient for intrinsic ATP hydrolysis activity (Figure 5) displayed the same proteolysis pattern seen for wild-type Kar2 in the presence of ATP (Figure 6e, ATP). The majority of these alleles also showed proteolysis patterns similar to those observed for wild-type Kar2 when incubated with ADP (Figure 6e, ADP). An exception was Kar2-C63I, which exhibited a proteolysis pattern in the presence of ADP that was almost identical to that observed in the absence of nucleotide (Figure 6e, ADP and no nucleotide), suggesting an altered interaction (binding and/or positioning) of ADP with the Kar2-C63I mutant. Several of the ATP hydrolysis deficient Kar2 mutants were capable of an ATP-dependent conformational change, including Kar2-C63H and Kar2-C63N (Figure 6c, ATP) and Kar2-C63K, Kar2-C63L, Kar2-C63M, Kar2-C63Q (Figure 6d, ATP). These data suggest these alleles are proficient for ATP binding, and capable of efficient allosteric communication between the nucleotide- and substrate-binding domains, yet deficient in nucleotide hydrolysis. A lower amount of protease-protected Kar2 fragments (weaker protein signal) was observed with Kar2-C63R (Figure 6c, ATP) and Kar2-C63E, Kar2-C63Y (Figure 6d, ATP) suggesting a somewhat compromised, but not absent, communication between domains upon ATP-binding in these mutants. However, further study showed all these ATP hydrolysis deficient Kar2 alleles were altered in their association with nucleotide relative to wild-type Kar2. Kar2-C63H, Kar2-C63N, Kar2-C63R (Figure 6c, ADP) and Kar2-C63E, Kar2-C63Y (Figure 6d, ADP) showed proteolysis patterns in the presence of ADP that were consistent with an absence of bound nucleotide (or an improperly positioned nucleotide). In the presence of ADP, the Kar2-C63L, Kar2-C63M, Kar2-C63Q mutants all showed increased recovery of full length Kar2 (like observed for wild type) yet all three proteins also displayed an increased level of SBD fragments, suggestive of an altered

interaction for these proteins with ADP (Figure 6d, ADP). The Kar2-C63K mutant showed banding patterns similar to those observed for wild-type Kar2 in the presence of nucleotide (ATP or ADP), however Kar2-C63K continued to show fragments consistent in size with full-length, lidless and NBD pieces in the absence of nucleotide (Figure 6d). Previous studies demonstrated mutation of the corresponding cysteine in a cytosolic Hsp70 to lysine (Hsc70-C17K) resulted in a tighter interaction with nucleotide [31], and it is possible that the proteolysis pattern we observed for Kar2-C63K in the absence of exogenous nucleotide is due to purification of nucleotide-bound Kar2-C63K. No ATP- or ADP-induced conformational change was observed for the Kar2-C63P, Kar2-C63W (Figure 6c) or Kar2-C63D, Kar2-C63F (Figure 6d), which all showed limited ATPase activity (Figure 5). These alleles could be deficient for nucleotide binding, or these alleles may be able to bind nucleotide yet be compromised in domain communication. Interestingly, the absence or presence of a conformational change did not strictly correlate with whether a given allele was incapable or compromised in their ability to complement a *kar2*Δ strain (Figure 2).

Substitution of the Kar2 cysteine with His, Phe, Pro, Trp, Tyr allows for increased cell viability in the presence of oxidant

We reported previously that addition of select Kar2 Cys63 mutant alleles allows for enhanced cell viability during cellular oxidative stress [1, 2]. These prior experiments built upon our observation that a strain containing a *kar2-C63A* allele was compromised for growth in the presence of exogenous or endogenous oxidants, relative to a strain containing wild-type Kar2 [1]. These earlier data suggest a beneficial role for cysteine oxidation in cell proliferation during oxidative stress and that cells containing a Kar2 allele that cannot be oxidized (Kar2-C63A) are at a growth disadvantage during hyper-oxidizing conditions [1]. Further experiments revealed several Kar2 cysteine mutants (Kar2-C63D/F/Y/W), provided as an additional allele in combination with the genomic *kar2-C63A,* could restore growth during stress, which we attribute to an ability of these alleles to mimic the function of an oxidized Kar2 [1]. These mutant alleles were provided ectopically due to the compromised growth (or lethality) associated with the Kar2-C63D/F/Y/W alleles as the sole copy of cellular *KAR2* [1] (Figure 2).

Using assays similar to those described previously, we sought to determine whether any of the additional Kar2 Cys63 mutations we described here had properties that benefited cell growth during ER oxidative stress. To generate oxidative stress within the ER, we overexpressed a hyperactive allele of the Ero1 protein (Ero1*), which we have shown to be an effective means to generate an overly oxidized ER [1, 2, 32]. Since Ero1* is toxic to cells, we used an inducible Ero1* allele driven by the galactose (*GAL1*) promoter, which can be induced by growing cells in medium containing galactose as the carbon source. Similar to what we reported previously, we observed *kar2-C63A* cells containing a plasmid encoding wild-type Kar2 showed an enhanced cell viability after 18 h of Ero1* expression, relative to a strain containing plasmid expressing Kar2-C63A or a strain with an empty plasmid (Figure 7a), as indicated by the greater number of viable colony forming units recovered from the Kar2-expressing strain post-stress. We found an even more robust growth advantage was conferred by *kar2-C63H* and *kar2-C63P* alleles, as well as our previously reported *kar2-C63F/Y/W* alleles (Figure 7a), which all resulted in no measurable loss in cell viability upon

Ero1* expression. We suggest the enhanced viability for these strains relative to a strain with wild-type Kar2 reflects an optimal combination of unmodified Kar2 (Kar2-C63A, encoded by the genome) and a modified-Kar2 mimetic (e.g. Kar2-C63H/P from the introduced plasmid) in these strains, which genetically recapitulates the normally reduced and oxidized pools of Kar2 in the ER. Interestingly, all five of these strongly protective alleles showed a loss of basal and stimulated ATPase activity (Figure 5) and were compromised for growth when present as the sole copy of cellular *KAR2* (Figure 2). Notably, several of these five alleles showed a dominant-negative growth defect under non-stress conditions relative to the other *kar2-C63* alleles; this was apparent upon quantitation of cell numbers prior to induction of stress (Figure 7a, t=0), where the number of colony forming units recovered on these plates was lower than the other strains, despite plating the same quantity of cells (based on cell optical density measurements). We attribute the decreased colony numbers at time zero to a loss of viability over the two days cells are allowed to form colonies on the plates. These data account for the >100% viability attributed to these *kar2* alleles, which is calculated by normalizing the colony forming units recovered after 18 h to the cell number at time zero (Figure 7b). We previously reported a similar fitness disadvantage conferred to yeast by the presence of the *kar2-C63F* and *kar2-C63Y* alleles under non-stress conditions [2]. Building upon our prior observation, we anticipate the protection afforded by these alleles is a byproduct of enhanced ATP-independent chaperone activity, which is a consequence of structural alterations in the nucleotide-binding domain (caused by alteration of the cysteine) that are propagated to the peptide-binding domain. We suggest the dominant negative growth defects observed for these mutants are a consequence of enhanced holdase activity that may be detrimental to protein secretion under non-stress conditions.

In addition to these very strong protective alleles, we also observed a strong increase in cell viability with the *Kar2-C63D/G/K/M/Q/R* alleles during stress (Figure 7a, 7b). Again, the majority of these protective alleles showed compromised ATPase activity (Figure 5) and a limited ability to serve as the sole copy of *KAR2* (Figure 2). An exception was the increase in viability observed with the *kar2-C63G* allele, which maintains detectable basal and stimulated ATP-hydrolysis activity (Figure 5). Although loss of ATPase activity did appear as a common characteristic among the protective alleles, we observed a loss of ATP-hydrolysis activity was not sufficient to confer protection during oxidative stress; ATPase-deficient mutants Kar2-C63E and Kar2-C63N (Figure 5) did not provide for increased viability upon hyper-oxidation of the ER (Figure 7a, 7b).

Most of the Kar2 mutants observed to be the least disrupted for ATPase activity (Figure 5) conferred no growth advantage during oxidative stress beyond that observed with Kar2-C63A (an exception being the Kar2-C63G, discussed above) (Figure 7a, 7b). We attribute the modest increase in viability (relative to vector alone) for the Kar2-C63A (and similar) strains to reflect some benefit provided by additional Kar2 ATPase activity (Figure 7b, purple). We suggest the further enhanced growth provided by wild-type Kar2 (Figure 7b, blue) and several Kar2 mutants (Figure 7b, red) relates to the changes in Kar2 activity that normally occur upon Kar2 cysteine oxidation and are mimicked by a subset of the Cys63 mutants. Together these data suggest several Kar2 cysteine mutants result in an altered function that is beneficial to cell growth during stress, which often is observed alongside a loss of ATPase activity.

We observed the subset of Kar2 Cys63 mutants that conferred a growth advantage during overexpression of Ero1* also showed an increased resistance to growth in the presence of the exogenous oxidant diamide. Specifically, cells were able to tolerate a higher concentration of diamide on plates (exhibited a decreased zone of growth inhibition) if they contained an ectopic allele of *kar2-C63F, kar2-C63H, kar2-C63Q, kar2-C63W, kar2-C63Y* (Figure 7c). However, we did not observe significant growth enhancement for cells exposed to diamide containing an ectopic allele of *kar2-C63P* (Figure 7c), which was strongly protective against Ero1* overexpression. This lack of apparent resistance to diamide could be a consequence of the dominant-negative growth impact we observed for this allele in the prior assay (Figure 7a, 7b); a *kar2-C63W* allele (which showed a dominant-negative impact on cell growth under non-stress conditions) was also less protective in the diamide assay than was anticipated relative to the strong growth enhancement observed in cells overexpressing Ero1* (Figure 7). We expect the halo assay, where cells are introduced gradually to diamide as it diffuses through the plate, may result in a situation that obscures the growth enhancement for these alleles that are dominant-negative under non-stress conditions. A more modest improvement in the ability to grow in the presence of diamide was observed with the *kar2-C63K/M/R* alleles. In addition, a modest growth enhancement in the presence of diamide was seen for cells containing *kar2-C63I*; this allele did not facilitate increased survival of cells exposed to the endogenous oxidant Ero1* (Figure 7). Altogether, these two assays identify eight alleles that confer a growth enhancement to cells exposed to exogenous (diamide) or endogenous (Ero1*) oxidant: three alleles identified previously (*kar2-C63F/Y/W)* and five new alleles (*kar2-C63H/K/R/P/Q).* We also observed more modest protection conferred by several additional mutants, including Kar2-C63D that we previously reported to show protective activities [1, 2]. However, we specifically highlight these eight Kar2 mutants, which show a robust ability to restore growth during oxidative stress even in the absence of significant ATPase function.

DISCUSSION

We suggest the strong conservation of a cysteine within the BiP ATPase domain reflects a unique set of properties rendered by the cysteine side chain, which cannot be replicated in full by the other 19 common amino acids (summarized in Figure 8). We propose that the inability of other amino acids to fully recapitulate Kar2 function under reducing and oxidizing conditions relates to the unique physio-chemical properties of cysteine including: (i) a small side chain and (ii) susceptibility to post-translational oxidation. We anticipate it is these unique characteristics of cysteine that allow Kar2 to facilitate cell survival under a range of redox conditions.

Kar2 Cysteine and ATPase Activity

The relatively small size of the cysteine side chain appears to enable efficient ATP hydrolysis. In general, Kar2 proteins containing amino acids with smaller side chains in place of Cys63 retained ATP hydrolysis activity *in vitro* (Figure 5) and maintained the ability to complement a *kar2*Δ strain under standard growth conditions and heat stress (Figure 2). In contrast, amino acids with larger side chains were poorly tolerated at position 63 and resulted in Kar2 mutants with low (or no) ATP hydrolysis activity (Figure 5). These

mutants were also severely compromised in their ability to support yeast growth and viability (Figure 2). Kar2 Cys63 is located within the nucleotide-binding pocket in close proximity, but not in physical contact with, the bound nucleotide; the ADP-bound Kar2 ATPase domain structure shows the nucleotide α-and β-phosphate located approximately 8 and 8.5 Å from the Cys63 Cβ atom [25]. Given the relative distance between the cysteine and nucleotide, it is not surprising that addition of a larger side chain does not appear to simply occlude ATP binding. For example, the catalytically dead Kar2-C63H mutant maintains the ability to undergo an ATP-dependent conformational change (Figure 6a), suggesting an ability to bind ATP despite an absence of detectable ATP hydrolysis (Figure 5). Instead we anticipate that structural changes introduced by the larger side chains may more subtly impact the structure of the nucleotide-binding pocket, which could alter nucleotide hydrolysis, nucleotide affinity, and/or the allosteric communication between the NBD and SBD. Indeed, the altered interaction between ADP and several of the Kar2 alleles that appeared proficient for an ATP-dependent conformation change suggests an altered environment within the nucleotide-binding pocket (Figure 6). Interestingly, NBD structures for wild-type Hsc70 and the Hsc70 mutant containing Lys in place of the conserved Cys (Hsc70-C17K) have been solved, and these two proteins show identical tertiary folds [31]. Similar to what we observed for Kar2-C63K, the Hsc70-C17K mutant is severely compromised for ATP hydrolysis, yet this loss of hydrolytic activity does not manifest as a gross structural alteration [31]. Instead, the authors propose the severe hydrolysis defect observed for Hsc70-C17K may relate to the exclusion of a potassium ion from the active site [31]. Intriguingly, the Hsc70-C17K mutant shows the same low basal hydrolysis rate as wild-type Hsc70 with sodium bound; perhaps the Kar2 alleles that show negligible stimulated ATPase activity in our assays (in the presence of potassium) are able to support some yeast growth as the sole copy of cellular *KAR2* (e.g. Kar2-C63D/E/F/Y) due to a limited activity with other ions, which in combination with increased Kar2 levels through UPR-induction may allow for growth of these strains at low temperature despite a significant hydrolysis defect. Alternatively, these alleles may retain some residual ATPase activity (undetectable in our assay) that is effectively stimulated in vivo by the additional J proteins and/or NEFs found in the yeast ER, which were not tested in our in vitro assay.

It is noteworthy that several Kar2 mutants with Cys63 amino acid replacements comparable in size (or smaller) than cysteine also altered Kar2 activity. Yeast strains containing Kar2-C63G, Kar2-C63I, Kar2-C63S, Kar2-C63T (as the sole copy of Kar2) all showed an elevated UPR (Figure 4), and recombinant protein with these amino acids demonstrated a lower intrinsic rate of ATP hydrolysis (Figure 5c). Interestingly, ATP hydrolysis by the Kar2-C63I/T mutants was more strongly stimulated by J-protein (Sec63J) and dampened in the presence of a NEF (Lhs1) (Figure 5f). These data may reflect an altered positioning of nucleotide in the Kar2-C63I/T mutants that results in more facile hydrolysis in the presence of J protein; alternatively, changes to the binding pocket may facilitate larger structural alterations that modify the affinity toward Sec63J and Lhs1. The altered proteolysis pattern observed for the Kar2-C63I mutant in the presence of ADP is consistent with such an altered positioning of nucleotide for Kar2-C63I (Figure 6e). Only two Kar2 Cys63 mutants appeared virtually identical to wild-type Kar2 in assays dependent on ATPase activity: Kar2-C63A and Kar2-C63V. Both these amino acids are small and hydrophobic. Given the

location of Cys63 within the nucleotide-binding cleft, it seems appropriate that hydrophobic side chains would be well tolerated. Calculations of the accessible surface area (ASA) of the cysteine residue using the Kar2 NBD structures [25] and the PDBePISA service (http://pdbe.org/pisa/) suggest an ASA of ~ 2 Å. These data indicate that the cysteine is solvent accessible, in keeping with the cysteine's susceptibility to oxidation, yet suggest the cysteine is relatively buried in the protein active site.

Kar2 Cysteine and Oxidative Stress

In contrast to the advantages observed for a small hydrophobic side chain with respect to ATPase activity, it appears that disruption of the normal ATPase cycle as a consequence of additional bulk and/or charge at position 63 is what promotes enhanced viability during oxidative stress (Figure 7). We have demonstrated previously that Kar2 with an oxidized cysteine shows an increased association with polypeptides [1, 2]. Peptide dissociation by mammalian BiP has been shown to correlate with an ATP-dependent conformational change [29], and it is notable that several of the most protective Kar2 Cys63 mutants were structurally unresponsive to ATP: Kar2-C63P/R/W (Figure 6a) and Kar2-C63F/Y (Figure 6b). These data suggest that the protective effect for these mutants during oxidative stress correlates with a more extended interaction with polypeptides, like observed for oxidized Kar2. Although the absence of an ATP-dependent conformational change did correspond with protection during stress, not all protective alleles were unresponsive to nucleotide. For example, the Kar2-C63H/Q mutants showed an ATP-induced proteolysis pattern similar to wild-type Kar2 (Figure 6). These alleles may have a subtle defect toward nucleotide binding, as suggested by altered proteolysis pattern observed with Kar2-C63H in the presence of ADP (Figure 6c). Alternatively, these mutants may facilitate an increased association with polypeptides through a distinct mechanism. Of note, the Kar2-C63H mutant did show a dominant negative impact on cell growth during non-stress conditions (Figure 7), which we have attributed previously to an enhanced holdase activity that is detrimental to protein folding and secretion under normal growth [2].

We observed introduction of charge or bulk at Kar2 residue 63 alone is not sufficient to mimic Kar2 cysteine oxidation. The Kar2-C63E and Kar2-C63N mutants are severely compromised for ATPase activity yet these alleles did not show an ability to promote cell growth during oxidative stress. These data with Kar2-C63E/N support our prior observation that a loss of ATPase activity (due to a T249G mutation) is insufficient to protect cells during oxidative stress [1]. The Kar2-C63E and Kar2-C63N mutants also both showed a conformational change in the presence of ATP (Figure 6), which is consistent with (although not proof of) a lack of enhanced holdase activity for these alleles.

Kar2 (BiP) Orthologs

Our database search for BiP orthologs revealed sequences in entamoebae and trypanosmes that lacked the conserved cysteine within the ATPase domain present in Kar2 and the majority of BiP orthologs (Figure 1). Sequences were identified in *E. histolytica* (**XP_653218**), *E. nuttalli* (**XP_008855870**), *E. dispar* (**XP_001738012**), and *E. invadens* (**XP_004183988**), which all contained an alanine in place of the cysteine. BiP sequences in *T. brucei* (**AAC37174**), *T. cruzi* (**EKG01171**), *T. rangeli* (**ESL08562**), *T. grayi*

(**XP_009308651**), *T. vivax* (**CCD20294**), and *T. congolense* (**CCD11770**) all showed a valine in substitution for the cysteine. Of interest, these are the two amino acid substitutions for Kar2 that showed unperturbed ATPase activity, suggesting that the absence of the cysteine in these BiP orthologs will not impact their function as an ATPase. However, the absence of a cysteine in these BiP orthologs suggests these organisms will lack the protective effects imparted by BiP oxidation.

Other redox pathways independent of BiP may compensate for a lack of BiP-mediated redox signaling in trypanosomes and entamoebae. Alternatively, both entamoebae and trypansomal BiPs contain other cysteines, and perhaps these cysteines are responsive to oxidant. Entamoebae BiPs contain two cysteines; one cysteine is located within the predicted signal sequence and a second is present within the last 50 amino acids of the peptide-binding domain, which normally forms a dynamic lid that controls peptide binding. It seems unlikely the first cysteine would serve as a redox sensor. However, it is exciting to speculate that modification of the second cysteine could alter lid dynamics, in turn enhancing the affinity toward polypeptides similar to what we have reported for oxidation of Kar2 Cys63. Notably, point mutations in the analogous lid region of the bacterial Hsp70 DnaK have been shown to enhance DnaK chaperone activity [33]. Trypanosomal BiPs also contain two cysteines, both located within the ATP-binding domain. One cysteine is analogous to Kar2 Ala312, which is located on an inner surface of a helix in lobe IIB [25]. Although this cysteine appears relatively buried in Kar2, it is interesting that a cysteine at the same position the primary sequence is present in the arabidopsis BiP orthologs, and this cysteine could be redox active. More intriguing is the second cysteine, which is close in primary sequence to the Kar2 Cys63 (Figure 1) and is positionally equivalent to Kar2 Val52, which is found on the BiP surface close in space to the polypeptide linker that connects the NBD and SBD [25]. Interestingly, this dynamic linker is known to be important in domain communication, which modulates peptide binding. Thus, it seems possible that oxidation of this cysteine in trypanosomal BiP during oxidative stress could modulate peptide binding, allowing for protection during oxidative stress. Alternatively, the Kar2-C63V allele did exhibit some protective capacity during oxidative stress induced by overexpression of Ero1* (Figure 7); it may be that the valine in place of cysteine in trypanosomal BiP is sufficient to promote beneficial chaperone activities associated with unmodified and oxidized cysteine in the other BiP orthologs.

In addition to the BiP orthologs, the ATPase domain cysteine is found the eukaroytic cytosolic Hsp70s (such as Hsc70) and is also well conserved in the bacterial Hsp70 DnaK. Like observed for BiP, redox modification of the conserved cysteine in DnaK occurs upon cellular exposure to oxidant, yielding sulfenic and/or glutathione adducts [34, 35]. Intriguingly, a database search for DnaK orthologs revealed DnaK proteins exist that lack the highly conserved cysteine and instead contain an alanine or valine at the corresponding position (similar what is seen for the BiP orthologs). For example, DnaK in the firmicute *S. agalactiae* (**P0A3J2**) contains an alanine while cyanobacteria *G. violaceus* DnaK (**Q7NDH1**) and the actinobacteria *S. avermitilis* DnaK (**Q826F6**) contain a valine. The later two DnaKs contain an additional cysteine that could be redox active, yet the *S. agalactiae* DnaK does not contain any cysteines. However, for bacteria it has been suggested that while

oxidation of the cysteine may contribute toward the inactivation of DnaK ATPase activity during oxidative stress, oxidation is not required for inactivation; instead, it has been proposed that inactivation is primarily a consequence of low nucleotide levels during oxidative stress [34]. Thus the absence of a cysteine in DnaK in certain bacteria may still allow for beneficial inactivation of DnaK during oxidative stress conditions.

In the long term, it will be interesting to ascertain whether BiP orthologs that lack the strikingly conserved cysteine within the ATPase domain rely on other cysteines to modulate chaperone activity during oxidative stress. In addition, it will be exciting to elucidate the similarities and differences between the redox-signaling events mediated by invertebrate and vertebrate BiP orthologs; the striking conservation of a second cysteine among the vertebrate orthologs (Figure 1) suggests the capacity for disulfide bond formation during oxidative stress may be a unique BiP feature shared by vertebrate BiP orthologs. Whether vertebrate BiPs require both cysteines for enhanced chaperone activity during stress remains to be determined. Finally, how redox modification of BiP relates to the additional post-translational modifications described for BiP remains an unexplored question. We observed changes in the conformational dynamics for Kar2 alleles that behave like oxidation mimetics and confer a protective activity during oxidative stress (Figures 6, 7). Intriguingly, the efficiency of AMPylation and the propensity to form oligomers both appear to be altered based on the conformation adopted by BiP [15, 17]. Together these data suggest the possibility that BiP cysteine oxidation could impact and/or excluded AMPylation, and/or modulate the pool of BiP oligomers, providing additional layers of regulation for BiP activities.

MATERIALS AND METHODS

Plasmid and Strain Construction

Plasmids used in this study are listed in Table 1. Construction of Kar2 expression plasmids for yeast (pCS681) and bacteria (pCS817) has been described previously [1]. QuikChange mutagenesis was used to generate cysteine amino acid substitutions with a pCS681 or pCS817 template (Agilent Technologies, Santa Clara, CA). All mutations were confirmed by sequencing. To make pHS130, sequence coding for Lhs1 (residues 21-877) was PCR amplified from yeast genomic DNA and appended with a glycine-linker and StrepII tag (DNA sequence: GGA TCC GGC GGC GGA GGG TGG AGC CAC CCG CAG TTC GAA AAG). The Lhs-StrepII DNA fragment was inserted behind the NheI site in pET-28a (EMD Millipore, Billerica, MA), creating an in-frame fusion with sequence coding for an N-terminal His_6-tag.

Saccharomyces cerevisiae strains were grown and genetically manipulated using standard techniques. YPD is rich medium with 2% glucose. Synthetic minimal medium (SMM) contains yeast nitrogen base, an amino acid supplement mixture, and a carbon source: 2% glucose (SMM) or 2% galactose (SMM Gal). Uracil or leucine medium supplements were removed to select for plasmids as needed. Yeast strains used in this study are listed in Table 2. Construction of CSY214 and CSY278 is described in [1]. Plasmid covered genomic *KAR2* null strains were generated by transformation of CSY214 with the appropriate *LEU2* plasmid, followed by counter-selection of pCS623 on SMM with 5-fluoroorotic acid (5-

FOA) [36]. To ensure complete loss of the *URA3* pCS623 plasmid, mutant strains were struck onto 5-FOA plates twice before a final transfer to YPD plates. A minimum of three colonies per yeast strain was analyzed for phenotypic outcomes.

In vitro protein assays

GST-Sec63J and His_6-tagged Kar2 (residues 42-682) were purified using the buffers and conditions described previously [1]. For Kar2, 0.1 L of induced culture was loaded onto 0.1 ml Ni-IDA spin columns (BioVision, Milpitas, CA). Purified Kar2 proteins were exchanged into 10 mM Tris-HCl, pH 7.4, 50 mM NaCl, 10% glycerol by dialysis with DiaEasy Dialyzer system with a 6–8 kDa molecular weight cutoff (BioVision). His_6/StrepII-tagged Lhs1 protein was expressed and purified from BL21 (DE3) pLysS cells. Bacteria containing pHS130 were grown overnight to saturation at 37°C in LB medium containing 100 μg/ml ampicillin and 34 μg/ml chloramphenicol, and cells were diluted 1:80 in LB with antibiotics and grown for 2.5 h at 37°C. Cells were shifted to 18°C for 30 min prior to protein induction with 0.4 mM isopropyl-β-D-thiogalactopyranoside (IPTG) final overnight at 18°C. Cells were harvested, and cell pellets were solubilized with 10 ml lysis buffer (50 mM HEPES, pH 8, 0.3 M NaCl, 0.1 M KCl, 0.5% Triton-X-100, 10% glycerol, 10 mM imidazole) plus 1 mM PMSF, 1 μM pepstatin A, and 5 mM beta-mercaptoethanol (BME) per 1 L of cell culture. Cells were treated with lysozyme and lysed by sonication. Insoluble material was removed by centrifugation at 16,000 × *g* for 30 min. Soluble material was loaded onto a HiTrap chelating column charged with nickel, and the column was washed with 10 column volumes (cv) of lysis buffer. The column was subsequently washed with (i) 10 cv of wash buffer (50 mM HEPES, pH 7.4, 0.3 M NaCl, 5% glycerol, 10 mM imidazole) supplemented with 1% Triton-X-100, (ii) 10 cv of wash buffer with a final concentration of 1 M NaCl, (iii) 10 cv of wash buffer lacking glycerol and containing 10 mM $MgCl_2$ and 5 mM ATP, and (iv) 10 cv of wash buffer with 0.5 M Tris-HCl, pH 7.4. Protein was eluted with wash buffer containing 25 mM imidazole final. Proteins were concentrated and buffer was exchanged to 10 mM Tris-HCl, pH 8, 50 mM NaCl, 10% glycerol using a vivaspin-30 column (GE Healthcare). Protein concentrations were determined using a BCA protein assay (Thermo Fisher Scientific, Waltham, MA) with bovine serum albumin as a standard. Proteins were flash frozen in liquid nitrogen and stored at −80°C.

To measure intrinsic ATPase activity, 1 μM Kar2 was mixed with 50 μM cold ATP and 0.01 μCi/μl of hot [alpha-^{32}P]ATP (Perkin-Elmer, Waltham, MA) in ATPase buffer (50 mM Tris-HCl, pH 7.4, 50 mM KCl, 5 mM $MgCl_2$, 1 mM DTT) at room temperature. To measure stimulation of Kar2 activity, the reaction was supplemented with a final concentration of 1.5 μM GST-Sec63J and 1 μM Lhs1. At the indicated time points, aliquots were removed and activity was quenched with addition of an equal volume of 2X stop solution (0.14% SDS, 32 mM EDTA, 0.2 M NaCl). Samples were spotted onto polyethyleneimine cellulose TLC plates, and plates were developed in 1 M formic acid and 0.5 M LiCl. Conversion of ATP to ADP was imaged with a phosphorimager and quantified using the ImageQuant TL software package (GE Healthcare, UK).

The partial proteolysis of Kar2 was completed in a buffer of 20 mM HEPES, pH 7.4, 50 mM KCl, 2 mM $MgCl_2$, 0.1 mM EDTA, 1 mM DTT. Note, an additional 15 mM NaCl and 3%

glycerol were present in the final reaction, contributed by the buffer used for the recombinant Kar2 preparation. A total of 12.5 μg of Kar2 and 2 mM ATP were incubated in a final volume of 25.5 μl for 1 h at 37°C. TPCK-treated trypsin (0.14 μg) was added, and samples were incubated for an additional hour at 37°C. Buffer was added in place of protease for control samples. Reactions were quenched with final concentration of 8.5 mM PMSF and samples were incubated at room temperature for 15 min. Proteins were solubilized by addition of an equal volume of 2x sample buffer (125 mM Tris-HCl, pH 6.8, 20% glycerol, 4% SDS, 0.02% bromophenol blue) and a final concentration of 25 mM dithiothreitol (DTT). Proteins (~ 1 μg of initial Kar2 material) were separated using a 10% SDS-polyacrylamide gel, and proteins were visualized using a SYPRO Ruby stain.

Unfolded protein response (UPR) detection

CSY214-derived yeast strains, transformed with the UPRE-*lacZ* reporter plasmid pCS852 [1], were grown in SMM-ura-leu medium at 24°C overnight to saturation. Cells were diluted to an OD_{600} of 0.2 in SMM-ura-leu medium, cultures were grown for 4 h at 24°C, at which time a subset of samples were moved to a 37°C water bath for 1.5 h prior to harvest. A CSY289 sample treated with 2 mM DTT for 1.5 h at 37°C served as a positive control. Three plasmid transformants were assayed in duplicate for each strain. Cells were permeabilized using Y-PER (Thermo Scientific), and beta-galactosidase activity in cell lysates was quantitated as described [37].

Translocation westerns

CSY214-derived yeast strains were grown overnight to saturation in YPD at 24°C, the next day cells were diluted to an OD_{600} of 0.15 in fresh YPD, and cultures were incubated at 24°C until an OD_{600} of approximately 0.5 was reached. Cultures were divided, and half were moved to a 37°C water bath shaker. After 1 h, 5 OD_{600} units of cells were harvested, and lysates were prepared as described [38]. Samples were suspended in 120 μl of 1X sample buffer with 2% BME, and proteins were separated by SDS-PAGE (7.5%). Proteins were detected after transfer to a nitrocellulose membrane using appropriate antiserum and a HRP-conjugated secondary antibody. Chemiluminescent signals were detected with a ChemiDoc MP System (Bio-Rad).

Growth assays

CSY278 cells containing plasmids encoding various *KAR2* alleles were grown overnight at 30°C in glucose medium (SMM) to saturation. The following evening, cells were subcultured to an OD_{600} of 0.04 in SMM Gal medium to induce Ero1* expression. Cells, 5×10^{-5} OD_{600} units, were removed from the SMM Gal culture at the time of subculturing and spread onto SMM plates to assess strain viability. Liquid cultures were returned to 30°C, and 18 h later an additional 5×10^{-5} OD_{600} units of cells were removed and plated on SMM plates. Plates were incubated for 2 d at 30°C, and colony forming units were counted using the ImageQuant TL software package. For halo assays, lawns of 0.09 OD_{600} units (~2×10^6 cells) were plated on SMM-leu plates, and 15 μl of 1 M diamide was applied to a 6 mm filter disk placed in the center of the lawn. Plates were incubated for 2 d at 30°C.

Acknowledgments

We thank Kevin Thorsen for assistance with plasmid construction and protein expression. We acknowledge funding support from Cornell University and the National Institutes of Health (GM105958) to C.S.S.

ABBREVIATIONS

ER	endoplasmic reticulum
FL	full length
NBD	nucleotide-binding domain
NEF	nucleotide-exchange factor
SBD	substrate-binding domain
UPR	unfolded protein response

References

1. Wang J, Pareja KA, Kaiser CA, Sevier CS. Redox signaling via the molecular chaperone BiP protects cells against endoplasmic reticulum-derived oxidative stress. eLife. 2014; 3:e03496. [PubMed: 25053742]
2. Wang J, Sevier CS. Formation and Reversibility of BiP Protein Cysteine Oxidation Facilitate Cell Survival during and post Oxidative Stress. J Biol Chem. 2016; 291:7541–7557. [PubMed: 26865632]
3. Flynn GC, Pohl J, Flocco MT, Rothman JE. Peptide-binding specificity of the molecular chaperone BiP. Nature. 1991; 353:726–730. [PubMed: 1834945]
4. Behnke J, Feige MJ, Hendershot LM. BiP and its nucleotide exchange factors Grp170 and Sil1: mechanisms of action and biological functions. J Mol Biol. 2015; 427:1589–1608. [PubMed: 25698114]
5. Melnyk A, Rieger H, Zimmermann R. Co-chaperones of the mammalian endoplasmic reticulum. Subcell Biochem. 2015; 78:179–200. [PubMed: 25487022]
6. Nguyen TH, Law DT, Williams DB. Binding protein BiP is required for translocation of secretory proteins into the endoplasmic reticulum in Saccharomyces cerevisiae. Proc Natl Acad Sci U S A. 1991; 88:1565–1569. [PubMed: 1996357]
7. Vogel JP, Misra LM, Rose MD. Loss of BiP/GRP78 function blocks translocation of secretory proteins in yeast. J Cell Biol. 1990; 110:1885–1895. [PubMed: 2190988]
8. Kabani M, Kelley SS, Morrow MW, Montgomery DL, Sivendran R, Rose MD, Gierasch LM, Brodsky JL. Dependence of endoplasmic reticulum-associated degradation on the peptide binding domain and concentration of BiP. Mol Biol Cell. 2003; 14:3437–3448. [PubMed: 12925775]
9. Molinari M, Galli C, Piccaluga V, Pieren M, Paganetti P. Sequential assistance of molecular chaperones and transient formation of covalent complexes during protein degradation from the ER. J Cell Biol. 2002; 158:247–257. [PubMed: 12119363]
10. Nishikawa SI, Fewell SW, Kato Y, Brodsky JL, Endo T. Molecular chaperones in the yeast endoplasmic reticulum maintain the solubility of proteins for retrotranslocation and degradation. J Cell Biol. 2001; 153:1061–1070. [PubMed: 11381090]
11. Plemper RK, Böhmler S, Bordallo J, Sommer T, Wolf DH. Mutant analysis links the translocon and BiP to retrograde protein transport for ER degradation. Nature. 1997; 388:891–895. [PubMed: 9278052]
12. Hamman BD, Hendershot LM, Johnson AE. BiP maintains the permeability barrier of the ER membrane by sealing the lumenal end of the translocon pore before and early in translocation. Cell. 1998; 92:747–758. [PubMed: 9529251]

13. Walter P, Ron D. The unfolded protein response: from stress pathway to homeostatic regulation. Science. 2011; 334:1081–1086. [PubMed: 22116877]
14. Ham H, Woolery AR, Tracy C, Stenesen D, Krämer H, Orth K. Unfolded protein response-regulated Drosophila Fic (dFic) protein reversibly AMPylates BiP chaperone during endoplasmic reticulum homeostasis. J Biol Chem. 2014; 289:36059–36069. [PubMed: 25395623]
15. Preissler S, Rato C, Chen R, Antrobus R, Ding S, Fearnley IM, Ron D. AMPylation matches BiP activity to client protein load in the endoplasmic reticulum. eLife. 2015; 4:e12621. [PubMed: 26673894]
16. Sanyal A, Chen AJ, Nakayasu ES, Lazar CS, Zbornik EA, Worby CA, Koller A, Mattoo S. A novel link between Fic (filamentation induced by cAMP)-mediated adenylylation/AMPylation and the unfolded protein response. J Biol Chem. 2015; 290:8482–8499. [PubMed: 25601083]
17. Preissler S, Chambers JE, Crespillo-Casado A, Avezov E, Miranda E, Perez J, Hendershot LM, Harding HP, Ron D. Physiological modulation of BiP activity by trans-protomer engagement of the interdomain linker. eLife. 2015; 4:e08961. [PubMed: 26473973]
18. Chambers JE, Petrova K, Tomba G, Vendruscolo M, Ron D. ADP ribosylation adapts an ER chaperone response to short-term fluctuations in unfolded protein load. J Cell Biol. 2012; 198:371–385. [PubMed: 22869598]
19. Freiden PJ, Gaut JR, Hendershot LM. Interconversion of three differentially modified and assembled forms of BiP. EMBO J. 1992; 11:63–70. [PubMed: 1740116]
20. Wei PC, Hsieh YH, Su MI, Jiang X, Hsu PH, Lo WT, Weng JY, Jeng YM, Wang JM, Chen PL, Chang YC, Lee KF, Tsai MD, Shew JY, Lee WH. Loss of the oxidative stress sensor NPGPx compromises GRP78 chaperone activity and induces systemic disease. Mol Cell. 2012; 48:747–759. [PubMed: 23123197]
21. Altschul SF, Gish W, Miller W, Myers EW, Lipman DJ. Basic local alignment search tool. J Mol Biol. 1990; 215:403–410. [PubMed: 2231712]
22. Bangs JD, Uyetake L, Brickman MJ, Balber AE, Boothroyd JC. Molecular cloning and cellular localization of a BiP homologue in Trypanosoma brucei. Divergent ER retention signals in a lower eukaryote. J Cell Sci. 1993; 105:1101–1113. [PubMed: 8227199]
23. Field J, Van Dellen K, Ghosh SK, Samuelson J. Responses of Entamoeba invadens to heat shock and encystation are related. J Eukaryot Microbiol. 2000; 47:511–514. [PubMed: 11001149]
24. Marino SM, Gladyshev VN. Cysteine function governs its conservation and degeneration and restricts its utilization on protein surfaces. J Mol Biol. 2010; 404:902–916. [PubMed: 20950627]
25. Yan M, Li J, Sha B. Structural analysis of the Sil1-Bip complex reveals the mechanism for Sil1 to function as a nucleotide-exchange factor. Biochem J. 2011; 438:447–455. [PubMed: 21675960]
26. Kabani M, Beckerich JM, Brodsky JL. Nucleotide exchange factor for the yeast Hsp70 molecular chaperone Ssa1p. Mol Cell Biol. 2002; 22:4677–4689. [PubMed: 12052876]
27. Raynes DA, Guerriero V. Inhibition of Hsp70 ATPase activity and protein renaturation by a novel Hsp70-binding protein. J Biol Chem. 1998; 273:32883–32888. [PubMed: 9830037]
28. McClellan AJ, Endres JB, Vogel JP, Palazzi D, Rose MD, Brodsky JL. Specific molecular chaperone interactions and an ATP-dependent conformational change are required during posttranslational protein translocation into the yeast ER. Mol Biol Cell. 1998; 9:3533–3545. [PubMed: 9843586]
29. Wei J, Gaut JR, Hendershot LM. In vitro dissociation of BiP-peptide complexes requires a conformational change in BiP after ATP binding but does not require ATP hydrolysis. J Biol Chem. 1995; 270:26677–26682. [PubMed: 7592894]
30. Awad W, Estrada I, Shen Y, Hendershot LM. BiP mutants that are unable to interact with endoplasmic reticulum DnaJ proteins provide insights into interdomain interactions in BiP. Proc Natl Acad Sci U S A. 2008; 105:1164–1169. [PubMed: 18203820]
31. Wilbanks SM, McKay DB. Structural replacement of active site monovalent cations by the epsilon-amino group of lysine in the ATPase fragment of bovine Hsc70. Biochemistry. 1998; 37:7456–7462. [PubMed: 9585559]
32. Sevier CS, Qu H, Heldman N, Gross E, Fass D, Kaiser CA. Modulation of cellular disulfide-bond formation and the ER redox environment by feedback regulation of Ero1. Cell. 2007; 129:333–344. [PubMed: 17448992]

33. Aponte RA, Zimmermann S, Reinstein J. Directed evolution of the DnaK chaperone: mutations in the lid domain result in enhanced chaperone activity. J Mol Biol. 2010; 399:154–167. [PubMed: 20381501]
34. Winter J, Linke K, Jatzek A, Jakob U. Severe oxidative stress causes inactivation of DnaK and activation of the redox-regulated chaperone Hsp33. Mol Cell. 2005; 17:381–392. [PubMed: 15694339]
35. Zhang H, Yang J, Wu S, Gong W, Chen C, Perrett S. Glutathionylation of the Bacterial Hsp70 Chaperone DnaK Provides a Link between Oxidative Stress and the Heat Shock Response. J Biol Chem. 2016; 291:6967–6981. [PubMed: 26823468]
36. Boeke JD, Trueheart J, Natsoulis G, Fink GR. 5-Fluoroorotic acid as a selective agent in yeast molecular genetics. Methods Enzymol. 1987; 154:164–175. [PubMed: 3323810]
37. Guarente L. Yeast promoters and lacZ fusions designed to study expression of cloned genes in yeast. Methods Enzymol. 1983; 101:181–191. [PubMed: 6310321]
38. Kushnirov VV. Rapid and reliable protein extraction from yeast. Yeast. 2000; 16:857–860. [PubMed: 10861908]
39. Larkin MA, Blackshields G, Brown NP, Chenna R, McGettigan PA, McWilliam H, Valentin F, Wallace IM, Wilm A, Lopez R, Thompson JD, Gibson TJ, Higgins DG. Clustal W and Clustal X version 2.0. Bioinformatics. 2007; 23:2947–2948. [PubMed: 17846036]
40. Stothard P. The sequence manipulation suite: JavaScript programs for analyzing and formatting protein and DNA sequences. Biotechniques. 2000; 28:1102, 1104. [PubMed: 10868275]
41. Yang J, Nune M, Zong Y, Zhou L, Liu Q. Close and Allosteric Opening of the Polypeptide-Binding Site in a Human Hsp70 Chaperone BiP. Structure. 2015; 23:2191–2203. [PubMed: 26655470]
42. Qi R, Sarbeng EB, Liu Q, Le KQ, Xu X, Xu H, Yang J, Wong JL, Vorvis C, Hendrickson WA, Zhou L, Liu Q. Allosteric opening of the polypeptide-binding site when an Hsp70 binds ATP. Nat Struct Mol Biol. 2013; 20:900–907. [PubMed: 23708608]
43. Bertelsen EB, Chang L, Gestwicki JE, Zuiderweg ER. Solution conformation of wild-type E. coli Hsp70 (DnaK) chaperone complexed with ADP and substrate. Proc Natl Acad Sci U S A. 2009; 106:8471–8476. [PubMed: 19439666]
44. Taylor WR. The classification of amino acid conservation. J Theor Biol. 1986; 119:205–218. [PubMed: 3461222]

HIGHLIGHTS

- BiP (Kar2) contains a highly conserved cysteine within the ATPase domain
- Oxidation of the conserved cysteine can alter BiP's ATP-dependent chaperone activities
- BiP cysteine mutants can recapitulate unmodified or oxidized BiP activities
- No single amino acid replacement for cysteine can recreate all wild-type BiP functions
- Conservation of BiP's cysteine may reflect the unique properties imparted by cysteine

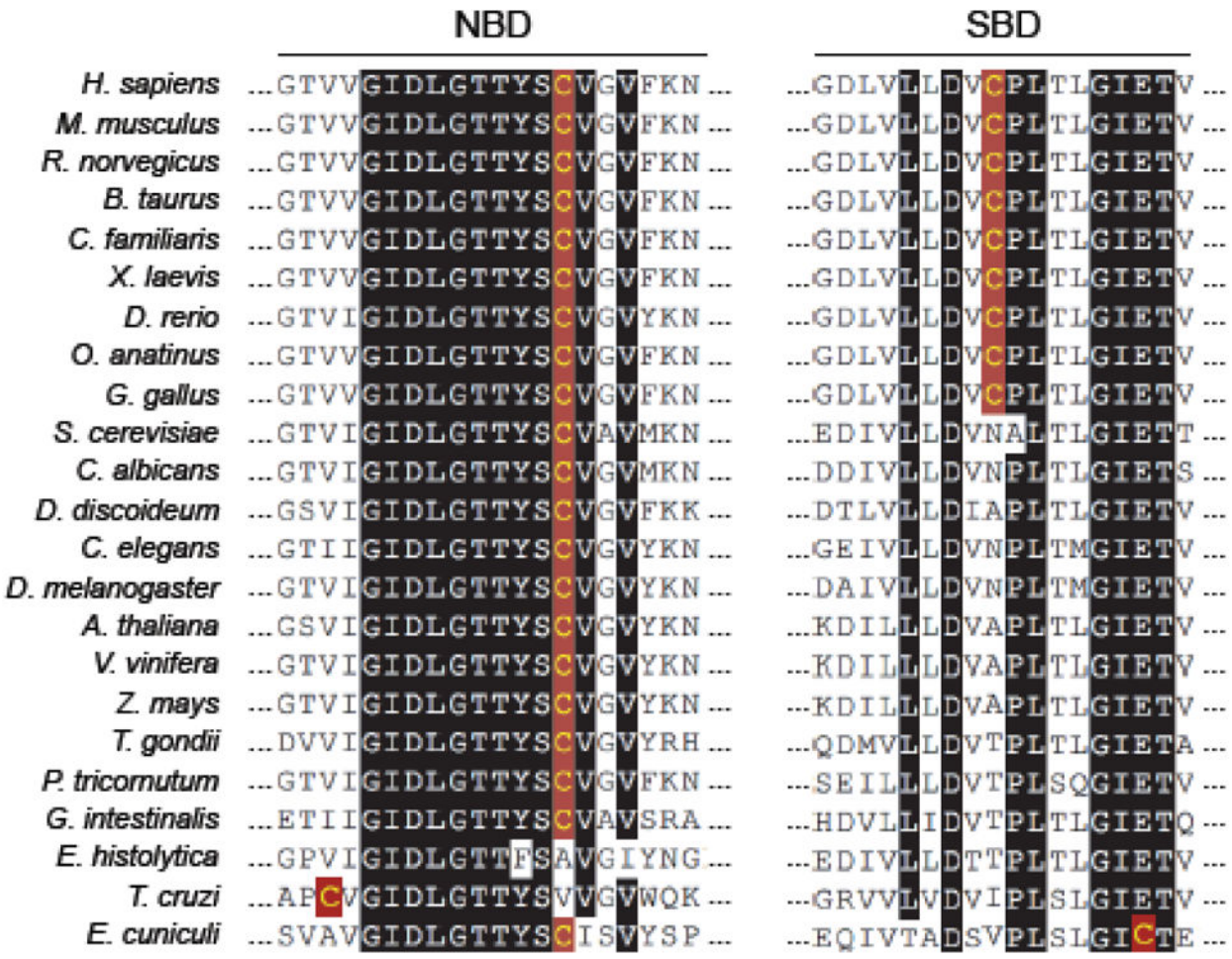

FIGURE 1.

Sequence alignment of BiP orthologs highlighting conserved cysteines. Protein sequences were aligned using ClustalW [39] and formatted using Multiple Align Show with a consensus-shading setting of 90% [40]. Cysteines are noted in red, independent of the consensus-shading threshold. Aligned residues include (from left to right) *M. musculus* amino acids 28–47 and 412–429, and *S. cerevisiae* amino acids 50–69 and 432–439, which are present within the nucleotide binding domain (NBD) and substrate binding domain (SBD) as indicated. These regions include the highly conserved redox-active cysteine described in *M. musculus* (Cys41) [20] and *S. cerevisiae* (Cys63) [1]. Also shown is *M. musculus* Cys420, which disulfide pairs to Cys41 during oxidative stress [20]. Aligned sequences were selected to span multiple taxonomic classes and include many commonly researched model organisms.

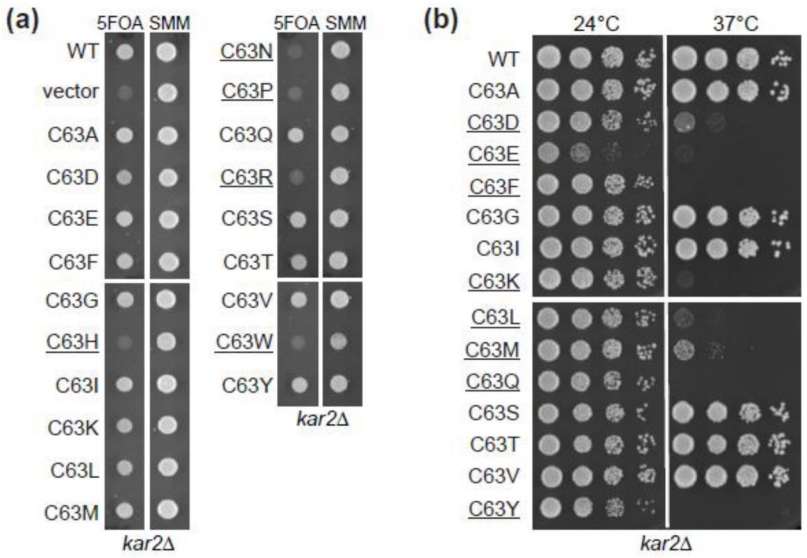

FIGURE 2.

Substitution of Kar2's cysteine disrupts cell viability. (**a**) Complementation of a yeast *kar2* deletion strain by Kar2 Cys63 alleles. CSY214 (*kar2*Δ [pCS623]) was transformed with *LEU2*-plasmids coding for the indicated Kar2 cysteine-substitution alleles (see Table 1). Yeast transformants were selected on SMM minus leucine and spotted onto SMM plates containing 5-FOA (to select against the wild-type *URA3*-marked *KAR2* plasmid pCS623) or SMM plates lacking leucine (to confirm effective transformation with the *LEU2*-marked *KAR2* plasmid). Viability was assessed after 3 d at 24°C. Underlined mutants highlight *KAR2* alleles unable to support viability of a *kar2*Δ strain. (**b**) Yeast strains from (**a)** that were viable on 5-FOA plates were grown overnight in YPD, spotted onto YPD plates, and incubated at 24°C for 3 d or 37°C for 2 d. Underlined mutants indicate *KAR2* alleles with a decreased capacity to support growth at high temperature (37°C) when present as the only copy of cellular *KAR2*.

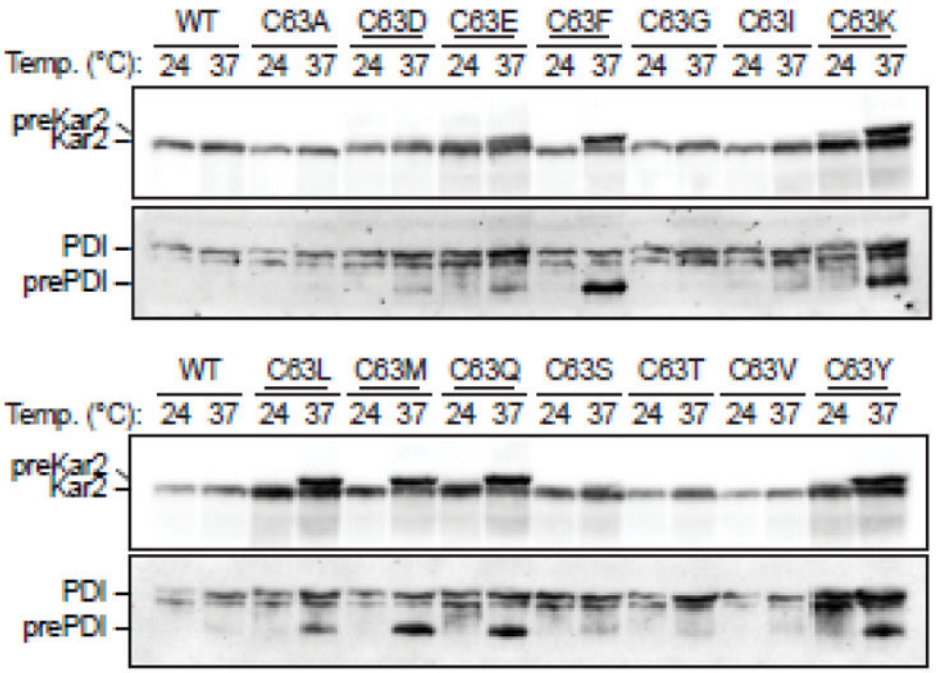

FIGURE 3.

Temperature-sensitive Kar2 mutant strains exhibit an attenuation of protein translocation. Yeast strains CSY289–296, 368, 400–405 were cultured in YPD at 24°C until mid-log phase. Cultures were either maintained at 24°C or shifted to 37°C for 60 min prior to harvest. Accumulation of untranslocated (unprocessed) forms of the proteins Kar2 and PDI was monitored by western blotting. Strains that show a temperature sensitive growth defect (Figure 2b) are underlined.

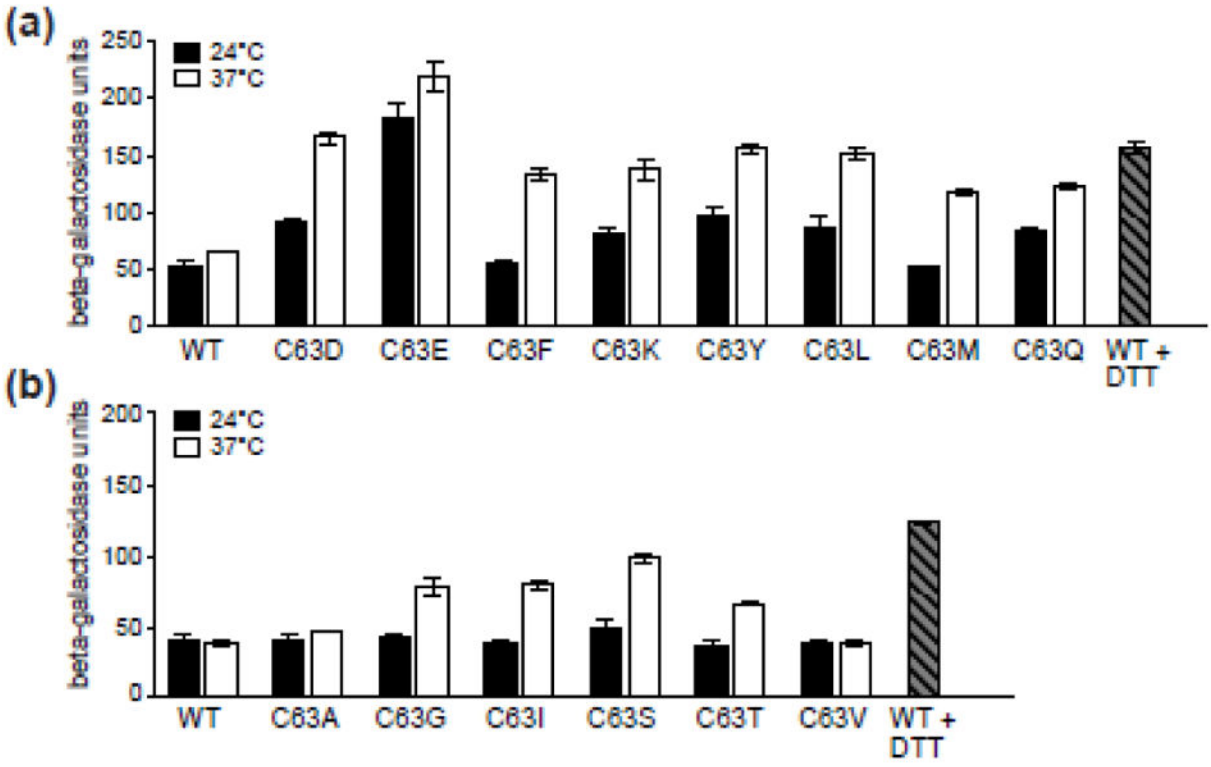

FIGURE 4.

A majority of Kar2 mutant strains show an elevated unfolded protein response (UPR). (**a**) Temperature-sensitive yeast strains CSY292–296, 368, 402, 403 and (**b**) yeast strains that do not show an obvious growth defect at high temperature (yeast strains CSY290, 291, 400, 404, 405) (see Figure 2b), along with the wild-type CSY289, were cultured at 24°C to log-phase in YPD and either maintained at 24°C or shifted to 37°C for 90 min (with or without 2 mM DTT). Three independent transformants of each strain were grown and assayed in duplicate. Data represent the mean of the averaged values for the three transformants ± SEM.

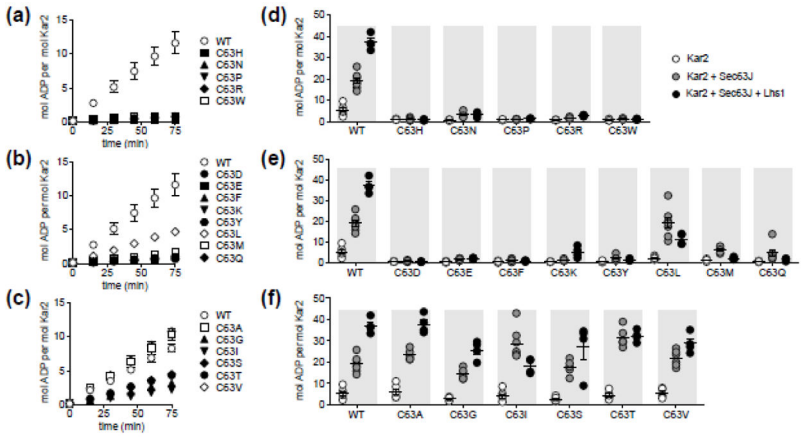

FIGURE 5.

Substitution of the Kar2 cysteine disrupts ATPase activity in vitro. Basal (**a–c**) and stimulated (**d–f**) Kar2 ATPase activities were assessed by following the fraction of [alpha-^{32}P]ATP converted to [alpha-^{32}P]ADP as described in the materials and methods. Samples in **d–f** were measured after 60 min. Data represent the mean of three independent assays ± SEM (**a–c**) or the mean of a minimum of four independent assays ± SEM (**d–f**). Kar2 proteins were assayed together in each independent experiment. For clarity, averaged data were separated and plotted as three groups based on the *in vivo* phenotypes observed for each mutant (described in Figure 2): (**a, d**) alleles unable to complement a *kar2*Δ strain, (**b, e**) alleles compromised in their ability to complement a *kar2*Δ (**c, f**), or alleles that show wild-type growth patterns. Wild-type data were repeated in each panel as a standard point of reference.

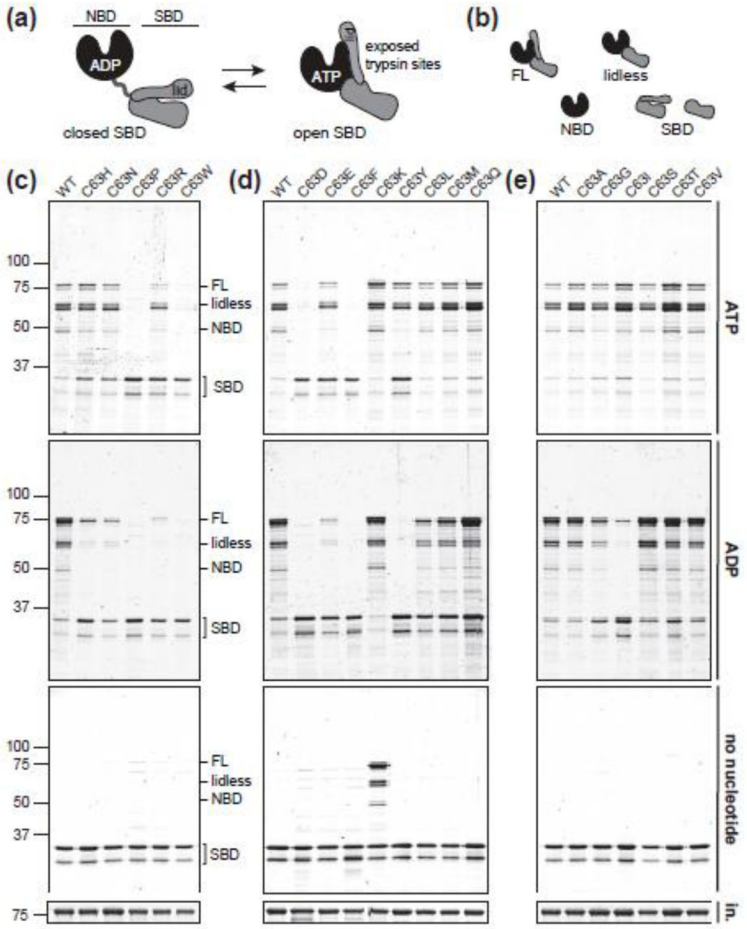

FIGURE 6.

A subset of Kar2 cysteine substitution mutants does not undergo nucleotide-induced conformational changes. (**a**) Cartoon depicting the conformational changes in the Kar2 substrate-binding domain (SBD) associated with nucleotide binding. Docking of the substrate-binding domain onto the nucleotide binding domain (NBD), associated with ATP binding, exposes protease sites otherwise inaccessible in the closed (undocked) state. Cartoons depict the conformations adopted with bound nucleotide as observed in the full-length structures of human BiP and the *E. coli* Hsp70 DnaK bound to ATP [41, 42] and DnaK bound to ADP (PDB 2KHO) [43]. (**b**) Depiction of the major proteolysis Kar2 fragments as deduced from their molecular weight and the presence (or absence) of the N-terminal histidine tag on recombinant Kar2. FL, full-length. (**c–e**) Wild-type or mutant Kar2 proteins were pre-incubated with ATP, ADP, or in the absence of nucleotide, for 1 h prior to digestion with trypsin (see materials and methods). Protein cleavage products were resolved by SDS-PAGE and visualized using a SYPRO protein stain. Protein not treated by protease was loaded as an assay control (labeled in. for input), and these samples are equivalent to ~25% of the material input into the protease assay. Protein samples are grouped based on the *in vivo* phenotypes observed for these mutant alleles (described in Figure 2): (**c**) alleles inviable as the only cellular *KAR2*, (**d**) alleles showing a temperature-sensitive growth defect as the only copy of cellular *KAR2*, or (**e**) alleles that show wild-type growth patterns.

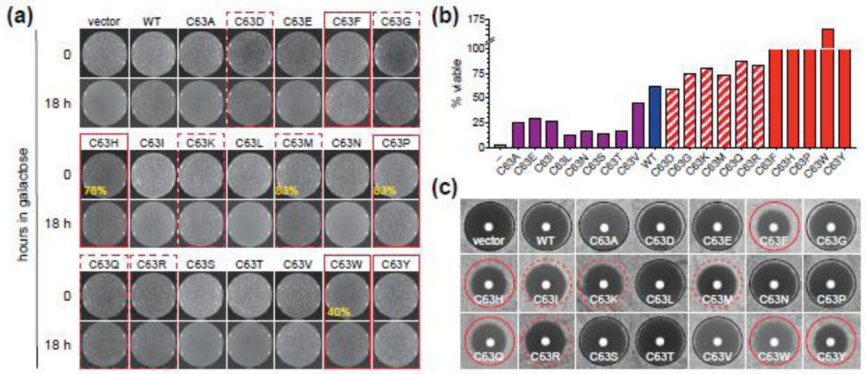

FIGURE 7.

Substitution of the Kar2 cysteine can enable protection against hyper-oxidation of the ER. (**a**) CSY278 containing plasmids encoding various *KAR2* alleles (see Table 1) were grown at 30°C in glucose medium (SMM) to saturation, at which time they were subcultured into galactose (SMM Gal) medium to induce Ero1* expression. Immediately after the switch to galactose medium (0 h), or after 18 h of growth in galactose, 5×10^{-5} OD units of cells were spread onto SMM plates to assess strain viability. Plates were photographed after 2 d at 30°C. Yellow percentages indicate the percent colonies observed for these strains at time 0 relative to the mean number of colonies observed across all the strains at time 0; percentages are shown for strains showing less than 90% the mean number of colonies. (**b**) Quantitation of plates in panel **(a)**. Colony forming units recovered after 18 h in galactose are express as percent colonies relative to the 0 h plate. Data shown are representative of two independent experiments. Red boxes (solid or dashed) in panel (**a)** correspond to the relative enhancement in viability represented numerically in panel (**b)** (red solid or hatched bars). (**c**) Strains from **(a)** were spread as a lawn on SMM plates, and diamide was applied to a filter disk in the center of the lawn. Plates were incubated at 30°C for 2 d. Plates shown are representative of two independent experiments. A black circle indicates the halo size observed for a strain containing empty vector. Strains showing an increased resistance to diamide (smaller halo size) are noted with a solid red circle (most diamide resistance) or with a red-dashed circle (a relatively weaker resistance to diamide, yet more diamide resistant than wild-type).

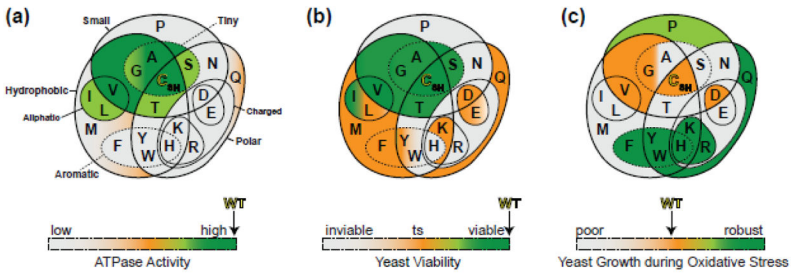

FIGURE 8.

Summary of Kar2 cysteine mutant properties. The 20 common amino acids are organized in a Venn diagram based on their side-chain properties according to the Taylor classification [44]. Diagrams are colored according the phenotypes observed when the Kar2 cysteine was substituted with the indicated amino acid for the Kar2 cysteine. Diagrams are shaded based on the impact on (**a**) ATPase activity, (**b**) the ability of Kar2 to serve as the only copy of cellular Kar2, and (**c**) the capacity of an ectopic Kar2 allele to confer enhanced viability during oxidative stress.

Table 1

Plasmids.

Name	Description	Markers	Source
pCS852	*UPRE-LacZ* reporter	*CEN URA3*	[1]
pCS452	P_{GAL1}-*ERO1*-myc*	*CEN URA3*	[32]
pCS623	*KAR2*	*CEN URA3*	[1]
pCS681	*KAR2*	*CEN LEU2*	[1]
pCS685	*kar2-C63A*	*CEN LEU2*	[1]
pCS802	*kar2-C63D*	*CEN LEU2*	[1]
pCS746	*kar2-C63E*	*CEN LEU2*	This study
pCS687	*kar2-C63F*	*CEN LEU2*	[1]
pCX1	*kar2-C63G*	*CEN LEU2*	This study
pCX2	*kar2-C63H*	*CEN LEU2*	This study
pCX3	*kar2-C63I*	*CEN LEU2*	This study
pCS749	*kar2-C63K*	*CEN LEU2*	This study
pCX4	*kar2-C63L*	*CEN LEU2*	This study
pCX5	*kar2-C63M*	*CEN LEU2*	This study
pCX6	*kar2-C63N*	*CEN LEU2*	This study
pCX7	*kar2-C63P*	*CEN LEU2*	This study
pCS747	*kar2-C63Q*	*CEN LEU2*	This study
pCX8	*kar2-C63R*	*CEN LEU2*	This study
pCS686	*kar2-C63S*	*CEN LEU2*	This study
pCX9	*kar2-C63T*	*CEN LEU2*	This study
pCX10	*kar2-C63V*	*CEN LEU2*	This study
pCS750	*kar2-C63W*	*CEN LEU2*	[1]
pCS688	*kar2-C63Y*	*CEN LEU2*	[1]
pCS817	His_6-*kar2-(42-682)*	KAN	[1]
pCS818	His_6-*kar2-(42-682)-C63A*	KAN	[1]
pCS822	His_6-*kar2-(42-682)-C63D*	KAN	[1]
pHS119	His_6-*kar2-(42-682)-C63E*	KAN	This study
pCS819	His_6-*kar2-(42-682)-C63F*	KAN	[1]
pHS88	His_6-*kar2-(42-682)-C63G*	KAN	This study
pCX20	His_6-*kar2-(42-682)-C63H*	KAN	This study
pHS89	His_6-*kar2-(42-682)-C63I*	KAN	This study
pCX23	His_6-*kar2-(42-682)-C63K*	KAN	This study
pHS90	His_6-*kar2-(42-682)-C63L*	KAN	This study
pHS91	His_6-*kar2-(42-682)-C63M*	KAN	This study
pHS92	His_6-*kar2-(42-682)-C63N*	KAN	This study
pCX21	His_6-*kar2-(42-682)-C63P*	KAN	This study
pKT1	His_6-*kar2-(42-682)-C63Q*	KAN	This study
pCX22	His_6-*kar2-(42-682)-C63R*	KAN	This study

Name	Description	Markers	Source
pCS851	*His_6-kar2-(42-682)-C63S*	KAN	This study
pHS94	*His_6-kar2-(42-682)-C63T*	KAN	This study
pHS95	*His_6-kar2-(42-682)-C63V*	KAN	This study
pCS821	*His_6-kar2-(42-682)-C63W*	KAN	[1]
pCS820	*His_6-kar2-(42-682)-C63Y*	KAN	[1]
pCS675	*GST-Sec63J*	AMP	[1]
pHS130	*His_6-lhs1-(21-877)- StrepII*	KAN	This study

Table 2

Yeast strains.

Strain	Genotype	Source
CSY278	*MATa GAL2 ura3-52 leu2-3,112 kar2-C63A can1::P_{GAL1}-ERO1*-myc*	[1]
CSY214	*MATa GAL2 ura3-52 leu2-3,112 kar2Δ::KanMX* [pCS623]	[1]
CSY289	*MATa GAL2 ura3-52 leu2-3,112 kar2Δ::KanMX* [pCS681]	[1]
CSY290	*MATa GAL2 ura3-52 leu2-3,112 kar2Δ::KanMX* [pCS685]	[1]
CSY368	*MATa GAL2 ura3-52 leu2-3,112 kar2Δ::KanMX* [pCS802]	[1]
CSY294	*MATa GAL2 ura3-52 leu2-3,112 kar2Δ::KanMX* [pCS746]	This study
CSY292	*MATa GAL2 ura3-52 leu2-3,112 kar2Δ::KanMX* [pCS687]	[1]
CSY400	*MATa GAL2 ura3-52 leu2-3,112 kar2Δ::KanMX* [pCX1]	This study
CSY401	*MATa GAL2 ura3-52 leu2-3,112 kar2Δ::KanMX* [pCX3]	This study
CSY296	*MATa GAL2 ura3-52 leu2-3,112 kar2Δ::KanMX* [pCS749]	This study
CSY402	*MATa GAL2 ura3-52 leu2-3,112 kar2Δ::KanMX* [pCX4]	This study
CSY403	*MATa GAL2 ura3-52 leu2-3,112 kar2Δ::KanMX* [pCX5]	This study
CSY295	*MATa GAL2 ura3-52 leu2-3,112 kar2Δ::KanMX* [pCS747]	This study
CSY291	*MATa GAL2 ura3-52 leu2-3,112 kar2Δ::KanMX* [pCS686]	This study
CSY404	*MATa GAL2 ura3-52 leu2-3,112 kar2Δ::KanMX* [pCX9]	This study
CSY405	*MATa GAL2 ura3-52 leu2-3,112 kar2Δ::KanMX* [pCX10]	This study
CSY293	*MATa GAL2 ura3-52 leu2-3,112 kar2Δ::KanMX* [pCS688]	[1]